American Journal of Ophthalmology Case Reports 41 (2026) 102514

Contents lists available at ScienceDirect

American Journal of Ophthalmology Case Reports

journal homepage: www.ajocasereports.com/

Cataract surgery with autosomal recessive cornea plana caused by a novel *KERA* mutation

Maram E.A. Abdalla Elsayed [a,b], Robert E. MacLaren [a,b,*]

[a] Oxford Eye Hospital, Oxford University Hospitals NHS Foundation Trust, Oxford, OX3 9DU, UK
[b] Nuffield Department of Clinical Neuroscience, University of Oxford, Oxford, OX3 9DU, UK

ARTICLE INFO

Keywords:
Cornea plana
KERA
Missense mutation
Cataract
Surgery

ABSTRACT

Purpose: To report a novel mutation in an autosomal recessive corneal plana with visually significant cataracts and a shallow anterior chamber.
Methods: Clinical ophthalmic examinations (including corneal topography and biometry) and direct sequencing of the *KERA* gene were performed.
Results: Genetic testing of a 92-year-old Caucasian gentleman with corneal plana revealed that the patient was homozygous for a *KERA* missense variant c.659T > C p.(Leu220Ser). This amino acid change occurs within a highly-conserved leucine-rich repeat in keratocan. The threedimensional structure of the keratocan protein was modelled, and the mutated position was found to be within the region of the leucine-rich repeat motifs, destabilizing the structure and leading to the classical ocular phenotype in the affected individual.
Scleralization of the cornea, flat keratometry, high astigmatism, and shallow anterior chamber depth make it challenging both for intraocular lens power calculation and cataract surgery. Phacoemulsification was successfully performed along with in-the-bag implantation of a 34D toric intraocular lens in one eye and a 34D plano lens in the other, resulting in a satisfactory refractive outcome.
Conclusion: Using protein modelling, a novel *KERA* mutation initially classified as variant of uncertain significance, could be identified as potentially pathogeneic. Biometry and cataract surgery in patients with corneal plana are challenging; however, a toric intraocular lens improves visual acuity.

1. Introduction

Autosomal recessive corneal plana (OMIM #217300) is a rare disorder characterized by peripheral scleralization and flattening of small corneas, resulting in a widened limbal zone, a decrease in corneal refractive power, and a shallow anterior chamber.

This disorder is caused by bi-allelic mutations in *KERA*. This gene encodes keratocan, an extracellular matrix and belongs to the Small Leucine-Rich Proteoglycans (SLRP) family, which comprises five distinct subfamilies.[1] They are a family of extracellular matrix proteins that are synthesized as a small core protein containing 6–20 leucine-rich repeat (LRR) motifs The highly conserved LRR motif consists of an 11-residue stretch, LxxLxLxxNxL, in which 'L' is Leu and 'N' is Asn. LRRs are flanked by cysteine clusters, a sulfur-containing amino acid that allows for disulfide bonds and the maintenance of the three-dimensional protein conformation, which plays a significant role in keratocan functioning. LRR motif alignment is thought to be vital in the uniform spacing of collagen fibrils (42–44 nm), on which corneal strength, transparency, and curvature are dependent. The gene spans 7.65 kilobases of genomic DNA, consists of three exons with complementary DNA of 2160 base pairs (bp), and encodes a protein of 352 amino acids. Exon 1 is untranslated, while exon 2 contains the start codon and an N-terminal signal peptide, followed by a highly conserved region containing 10 leucine-rich repeat (LRR) motifs.

We report the results of a molecular genetic analysis of *KERA* in a patient with corneal plana and suggest management options for intraocular lens measurement and cataract surgery in patients with this disorder.

2. Case history

A 93-year-old Caucasian male presented with bilateral, painless vision decrease after being referred by the optometrist for a reduction in vision. Clinical examination revealed best-corrected visual acuities of 6/

* Corresponding author. Oxford Eye Hospital, Oxford University Hospitals NHS Foundation Trust, Oxford, OX3 9DU, UK.
E-mail addresses: enquiries@eye.ox.ac.uk, Maram.abdalla@gmail.com (R.E. MacLaren).

https://doi.org/10.1016/j.ajoc.2026.102514
Received 24 November 2024; Received in revised form 29 December 2025; Accepted 31 December 2025
Available online 3 January 2026

36 and Count Fingers with +3.75D −2.50 @115° in the right eye and Count Fingers in the left eye. A +11.0 D balance lens had been used for the left eye due to amblyopia caused by high astigmatism. Apart from hyperopia and left amblyopia, there was no significant history of note. His siblings had passed away and he had no children. On examination, the pupillary responses were normal, there was an absence of a relative afferent pupillary defect, and intraocular pressures were within normal limits. He had an indistinct limbus, with a clear central cornea and shallow anterior chambers. Dense lens opacities were noted in both eyes (worse in the left eye), and iris architecture was normal. Fundal examination of the right eye revealed no remarkable findings. The posterior view of the left eye was hazy because of the cataract (Fig. 1). Corneal topography demonstrated abnormally low keratometry readings bilaterally (K1/K2 21.8/27.0 D in the right eye and K1/K2 19.4/28.7 D on the left). Q values measured −2.02 and 0.53 in the right and left eye respectively (Fig. 2). In addition, the left cornea was highly astigmatic (9.3 D) with an area of inferonasal ectasia. Central corneal thickness was low at 410 μm and 315 μm in the right and left eyes, respectively. Anterior chambers measured 1.15 mm in the right eye and 0.97 mm in the left eye. The axial lengths were 25.32 mm in the right eye and 25.55 mm in the left eye.

Informed consent for DNA blood sampling was obtained from the patient, and the samples were sent to Oxford Regional Genetics Laboratories. A custom-designed HaloPlex Target enrichment system (Agilent Technologies, Didcot, UK) was used to amplify the coding regions and intron/exon boundaries (± 10 bp) of the targeted genes, which were finally sequenced with an Illumina MiSeq instrument (Illumina, San Diego, CA, USA) at the High-Throughput Genomics Group at the Wellcome Trust Centre for Human Genetics, Oxford. The corneal dystrophy panel included the following genes: CHST6, COL17A1, COL8A2, DCN, GRHL2, GSN, KERA,

KRT12, KRT3, LCAT, MIR184, OVOL2, PIKFVE, PRDM5, SLC4A11, STS, TACSTD2, TCF4, TGFB1, UBIAD1, ZRB1, ZNF469. The detected variants were confirmed by Sanger sequencing.

Cataract surgery was advised for both eyes, starting with the left eye, to assess possible refractive outcomes and guide surgery of the dominant right eye. Due to the unpredictability of the zonules, surgery in the amblyopic eye would inform a superior approach in the better seeing eye. The amblyopic eye had very high astigmatism and it was therefore felt that to use a toric lens would be the best option hence, the lens with the highest available cylinder commercially available was used. The lens power was calculated using the SRK regression formula because of the inaccurate prediction of the post-operative lens position related to the out-of-range K values when using SRK/T. The required IOL power for the amblyopic left eye was beyond commercially available toric IOLs; hence, a +34.0 D +8.00 cyl Rayner lens was planned for the left eye and a 34 D plano lens for the right eye. In this case, a pragmatic approach was adopted and the highest power intraocular lens was implanted to avoid a piggy back lens in an eye which had a shallow anterior chamber.

Phacoemulsification was performed under topical anesthesia using intracameral lidocaine and epinephrine. VisionBlue® (trypan blue) and a vitrectomy light probe in the anterior chamber were used to aid in visualization. A combination of Viscoat (Alcon) and Healon GV (Abbott Medical Optics Inc., Santa Ana, CA) ophthalmic viscosurgical devices was used to protect the corneal endothelium and maintain the anterior chamber depth. A high bottle height, low flow parameters, and a stop-and-chop technique were used for nucleus removal. Owing to the unpredictable anatomy around the limbus and thin cornea, the corneal incision was closed using a 10–0 nylon suture.

Post-operative corneal edema resolved within the first month. However, the patient complained of a shape in his otherwise clear vision and underwent OCT imaging. This revealed macular neovascularization in the left eye with possible subretinal fibrosis, although it was difficult to clearly image through the cornea plana. One intravitreal injection of 2 mg/0.05 ml aflibercept was attempted; however, there was no response to treatment, which was assumed to be due to chronicity. The patient was satisfied with the visual improvement, and a similar procedure was performed in the right eye, but without using a toric lens because of the much lower astigmatism.

Post-operative cystoid macular edema was successfully treated with 0.5 % Ketorolac QDS.

The post-operative outcome was satisfactory, with best-corrected visual acuities of 6/12 (+1.25 0.50 @ 155 deg) in the right eye and 6/60 (−0.50D cyl @ 145) in the left eye due to preexisting amblyopia and macular neovascularization secondary to age-related macular degeneration. The refractive outcome in the left eye may have improved with earlier surgical intervention, which would have resulted in earlier detection of posterior neovascular activity.

2.1. Genetic testing

Genetic testing revealed that the patient was homozygous for the *KERA* missense variant c.659T > C p.(Leu220Ser), reported as a variant of uncertain significance. This variant has not been previously reported in ClinVar or GnomAD (accessed August 23, 2023). The *in silico* prediction program SIFT predicts the substitution to be pathogenic (SIFT score 0.00); however, Polyphen2 and MutationTaster2 predict the substitution to be benign.

2.2. Protein modelling

The crystal structure of human osteomodulin (Protein Data Bank

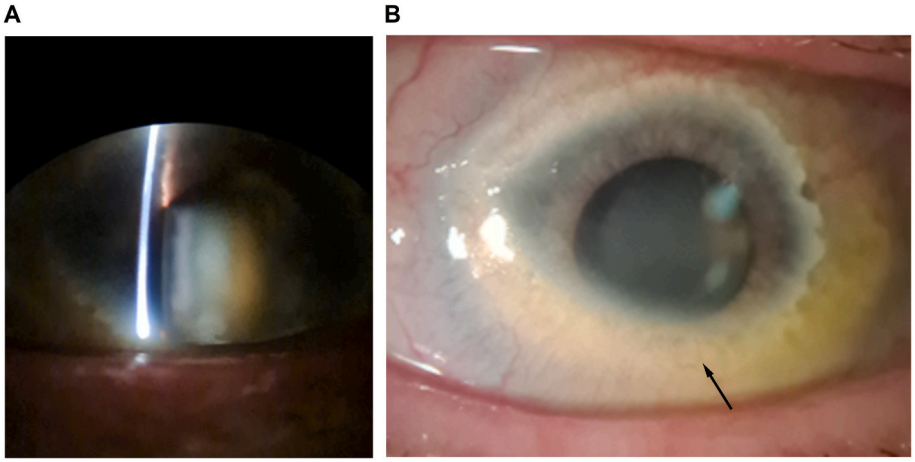

Fig. 1. Appearance of the left eye showing: **A.** Shallow anterior chamber and dense cataract; **B.** Indistinct limbus (black arrow) with a clear central cornea.

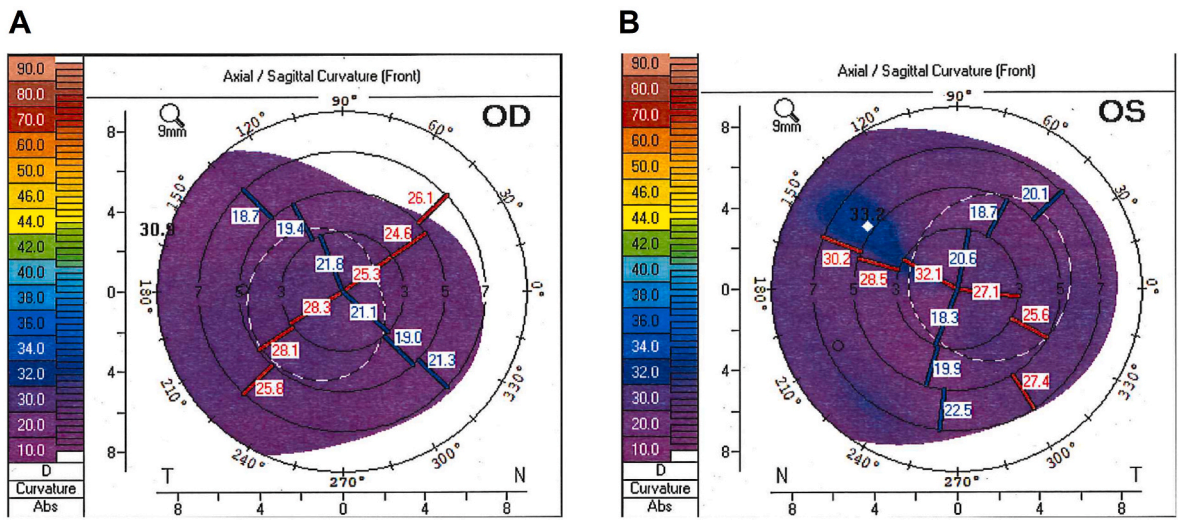

Fig. 2. Pentacam imaging in cornea plana showing the flat K readings and high astigmatism of the left eye.

accession no. 5YQ5) was used as a template to model the effects of the KERA Leu220Ser mutation using the PyMOL.

Molecular Graphics System (Version 1.2r3pre, Schrödinger, PyMOL) in combination with the PyMod plugin. Osteomodulin shares an overall 45.5 % homology with KERA at the amino acid level; however, it shares an identical leucine-rich repeat structure[2] which was used as a template because there is no published crystalline structure for KERA. To determine the importance of the WT Leu220 residue for KERA function, homology modelling was performed using the crystal structure of the human osteomodulin protein. This revealed that the WT Leu220 residue was located within the region encoding the leucine-rich repeat motifs (LRR), disrupting the 11 consensus motifs LXXLXLXXNXL. The substitution of the highly conserved WT Leu220 residue with a mutant Serine220 residue will change the hydrogen bond donor to a hydrogen bond acceptor or to neutral. Hence, the important stabilizing structure of the Asn ladder is likely disrupted (Fig. 3). Such perturbations can compromise the functional conformation of keratocan, potentially impairing its role in maintaining corneal transparency and extracellular matrix organization) describing how the identified structural changes may disrupt keratin's stability and intermolecular interactions. These disruptions could impair the protein's mechanical strength and structural integrity, offering a functional explanation for the pathogenic impact of the mutation.

The missense mutation found in this study was located within the leucine-rich repeat domain, which is essential for binding between keratocan and collagen fibrils in the corneal stroma during development. All missense mutations identified in the literature thus far are located in the leucine-rich repeat domains. The ExAC dataset showed that c.659T > C has not been detected in the general population. Aberrant KERA in the corneal stroma may not bind to collagen fibrils, consequently damaging the regulatory effect of KERA during the development of a normal corneal structure. The novel missense mutation in *KERA* exon 2 reported in the present study affects the sixth residue within the seventh LRR repeat, thereby disrupting the hydrophobic core.

3. Discussion

Here, we describe the clinical and genetic testing results of a patient with corneal plana. These findings expand the variant spectrum of the *KERA* gene, thereby providing mechanistic insights and facilitating genetic counselling. Furthermore, this highlights the challenges faced when calculating intraocular lens measurements and performing cataract surgeries in patients with this rare disorder.

To the best of our knowledge, the mutation reported appears to be the fifteenth *KERA* mutation to be reported and the seventh missense mutation to be described [1,3–6]. Hazy corneal appearance, flat corneas, and shallow anterior chambers of corneal plana patients are usually associated with short axial lengths and hyperopia; however, long axial lengths have been reported, as in the case presented. In the era of genetic testing, early diagnosis is critical not only for genetic counselling, but also for participation in clinical trials for cell and gene therapies with the potential to restore function and treat disease. Early clinical diagnosis is crucial for careful orthoptic assessment, refractive error management, and ametropic amblyopia prevention especially in a dominant disease which is incompletely penetrant. The identification of novel *KERA* mutations can enhance the diagnostic yield for corneal dystrophies with unclear genetic origins, thereby facilitating earlier and more accurate diagnoses. This information is crucial for genetic counselling, as it enables clinicians to provide affected families with more precise recurrence risk estimates and reproductive options. Moreover, these findings may support the development of targeted gene panels and inform future decisions regarding surveillance and management strategies in at-risk individuals.

Although successful cataract surgeries have previously been reported in corneal plana, neither case had excessively flat corneas or shallow anterior chambers, as in our patient.[7,8] Moreover, neither subject had a long axial length. Accurate prediction of post-operative refractive outcomes is crucial in cataract surgery planning, and the aim of this case was to leave the patient with a degree of hyperopia to enable him to enjoy an element of magnification from the spectacle lens prescribed post-operatively.

Even though the Haigis and Hoffer Q formulae have been shown to perform well in extremely hyperopic eyes following conventional biometry assessment, and phacoemulsification[9] extremely flat keratometry in corneal plana patients adds a significant hurdle in accurately calculating intraocular lens power. The online ASCRS calculator and IOLMaster™ (Carl Zeiss Meditec AG, Jena, Germany) could not be utilized for intraocular power calculations, as the corneal and anterior chamber depth measurements were outside the permissible or detectable range (in the case of the IOLMaster™). As a result, K readings from Pentacam were used in the intraocular power calculation. Pentacam images had to be manually captured, as the machine could not consistently locate the anterior corneal Purkinje image owing to the presence of dense cataracts and a poor tear film. The use of lubricants prior to image capture was not helpful. The average of the multiple scan readings was used to calculate the average K measurements for each eye. To cross-check the reliability of the IOL Master's astigmatism measurement,

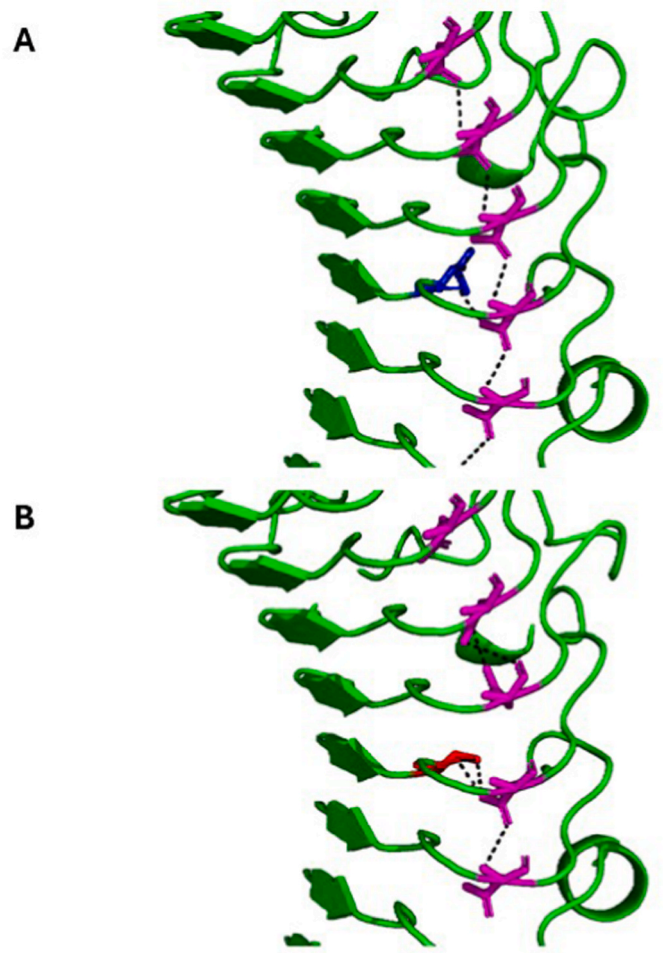

Fig. 3. The results of protein modelling**: A** shows a schematic representation of the leucin-rich repeat structure of the wild-type osteomodulin crystal structure (Leu220 is blue). **B** shows a three-dimensional model structure containing the Ser220 mutation in red. Asparagine is in magenta. Hydrogen bonds are in black. There is disruption of the repetitive pattern of hydrogen bonds with their neighbouring main-chain NH and CO groups thus resulting in disruption of the asparagine ladder that is vital for stability the parallel β-sheet-containing repeat proteins as it forms a ladder buried within the hydrophobic core. (For interpretation of the references to colour in this figure legend, the reader is referred to the Web version of this article.)

Javal-Schiotz keratometry was performed with a −1.00D lens to extend the scale allowing for estimation of flatter K readings beyond the instrument's normal range. This still only allowed capture of the steepest corneal meridien. Reassuringly, employing the astigmatism measurements suggested by Pentacam to estimate the flat meridien based on the Javal-Schiotz keratometer's steep meridian measurement provided mean K readings that were similar to those estimated by Pentacam.

The SRK formula was used giving an estimated intraocular lens measurement of 34.0 D. Although the SRK/T formula is commonly used as it predicts post-operative anterior chamber depth as a function of corneal curvature, axial length and the IOL A-constant,[10] errors are likely to arise in extremely hyperopic eyes as the algorithm's assumption of a correlation between axial length and anterior chamber depth no longer holds. Newer formulas such as Kane and EVO 2.0 outperform SRK/T, particularly in eyes requiring higher-powered lenses. For instance, Kane achieved a ±0.50 D accuracy rate of 58.8 %, followed closely by EVO 2.0 at 57.7 %, while SRK/T reached only 42.9 % in a cohort of eyes implanted with ≥30 D IOLs.[11]

A well-dilated pupil and light pipe made it easier to perform phacoemulsification on a grade 4 nuclear sclerotic cataract with a hazy cornea. Despite capsular stain with VisionBlue® (trypan blue) it was still difficult to visualize the anterior capsule due to the corneal opacities and irregular surface obscuring the red reflex. A vitrectomy light-pipe, placed via a limbal incision in the anterior chamber, was used to achieve retroillumination and optimal visualization. The surgeon also used a light pipe to manipulate the nuclear fragments and cortex.

Liberal use of Viscoat (Alcon Laboratories, Inc., Fort Worth, Texas, USA) protected the endothelium. To create and maintain space, a strongly cohesive ophthalmic viscosurgical device (OVD) Healon GV (Abbott Medical Optics Inc., Santa Ana, CA, USA) was used to deepen the anterior chamber. This improved maneuverability helped to flatten the anterior lens capsule. The infusion pressure was increased to its maximum level to deepen the anterior chamber. The combination of watertight incisions, liberal use of OVDs, and increased infusion pressure allowed maximum deepening of the anterior chamber.

In conclusion, we report a novel *KERA* variant in a patient with corneal plana and suggest management options for dealing with cataracts in such patients. Using bioinformatics software to manipulate protein structures determined by X-ray crystallography, we were able to predict a gene mutation, initially classified as a variant of uncertain significance, as being potentially pathogenic. This demonstrates the potential application of protein modelling as a tool to better inform the VUS interpretation of genetic tests, especially in cases where various *in silico* prediction programs provide conflicting results. Although patients with highly hyperopic cataract present unique challenges, meeting these challenges achieves satisfactory visual results, improves quality of life, and avoids missing potentially treatable posterior segment pathologies.

CRediT authorship contribution statement

Maram E.A. Abdalla Elsayed: Writing – review & editing, Writing – original draft, Investigation, Data curation. **Robert E. MacLaren:** Writing – review & editing, Validation, Supervision, Methodology, Conceptualization.

Patient consent

Written consent to publish this case has not been obtained. This report does not contain any personal identifying information.

Authorship

All authors attest that they meet the current ICMJE criteria for Authorship.

Funding

Oxford NIHR Biomedical Research Centre and Foundation Fighting Blindness Clinical Research Fellowship, USA.

Declaration of competing interest

The authors declare that they have no known competing financial interests or personal relationships that could have appeared to influence the work reported in this paper.

Acknowledgements

The authors would like to thank Sarah Howles, DPhil, MRCS (Eng), MA (Cantab), Nuffield Department of Surgical Sciences, University of Oxford, for her assistance in modelling the protein structure.

References

1. Pellegata NS, Dieguez-Lucena JL, Joensuu T, et al. Mutations in KERA, encoding keratocan, cause cornea plana. *Nat Genet.* 2000 May;25(1):91–95.

2. Tashima T, Nagatoishi S, Caaveiro JMM, et al. Molecular basis for governing the morphology of type-I collagen fibrils by osteomodulin. *Commun Biol*. 2018;1:33.
3. Ebenezer ND, Patel CB, Hariprasad SM, et al. Clinical and molecular characterization of a family with autosomal recessive cornea plana. *Arch Ophthalmol*. 2005 Sep;123(9):1248–1253.
4. Khan A, Al-Saif A, Kambouris M. A novel KERA mutation associated with autosomal recessive cornea plana. *Ophthalmic Genet*. 2004 Jun;25(2):147–152.
5. Kumari D, Tiwari A, Choudhury M, Kumar A, Rao A, Dixit M. A novel KERA mutation in a case of autosomal recessive cornea plana with primary angle-closure glaucoma. *J Glaucoma*. 2016 Feb;25(2):e106–e109.
6. Roos L, Bertelsen B, Harris P, et al. Case report: a novel KERA mutation associated with cornea plana and its predicted effect on protein function. *BMC Med Genet*. 2015 Jun 23;16:40.
7. Fogla R, Indumathy TR. Customized toric intraocular lens implantation in cornea plana. *J Cataract Refract Surg*. 2020 Dec;46(12):e11–e14.
8. Sutton G, Lawless MA, Rogers CM. Cornea plana. *Aust N Z J Ophthalmol*. 1995 Feb;23 (1):74–75.
9. MacLaren RE, Natkunarajah M, Riaz Y, Bourne RRA, Restori M, Allan BDS. Biometry and formula accuracy with intraocular lenses used for cataract surgery in extreme hyperopia. *Am J Ophthalmol*. 2007 Jun;143(6):920–931.
10. Retzlaff JA, Sanders DR, Kraff MC. Development of the SRK/T intraocular lens implant power calculation formula. *J Cataract Refract Surg*. 1990 May;16(3): 333–340.
11. Kane JX, Melles RB. Intraocular lens formula comparison in axial hyperopia with a high-power intraocular lens of 30 or more diopters. *J Cataract Refract Surg*. 2020 Sep;46(9):1236–1239.